Emission Spectroscopic Analysis of Poly(3-octyl thiophene) Exposed to Plasmas

Y. Rodríguez-Lazcano, H. Martínez

Instituto de Ciencias Físicas, Universidad Nacional Autónoma de México, Apartado Postal 48-3, 62210, Cuernavaca, Morelos, México

Received 28 August 2006; accepted 21 February 2007
DOI 10.1002/app.26509
Published online 16 May 2007 in Wiley InterScience (www.interscience.wiley.com).

ABSTRACT: Emission spectroscopy was employed to study reaction process of poly(3-octyl thiophene) (P3OT) exposed to helium, nitrogen, air and hydrogen plasmas. The plasma was generated by an AC discharge at a pressure of 2×10^{-2} Pa. The discharge power was maintained at an output of 220 V and a current of 0.2 A. The light emitted was monitored in the case of each plasma. Measurements at various discharge times were made of several emission peaks. The dominant emission bands were assigned to CH_2 at 589.32 nm, S_2 ($B^3\Sigma_u^- - X^3\Sigma_g^-$) at 413.35 nm, CH^+ ($A^1\Pi - X^1\Sigma$) at 422.51 nm and C_3H_3 at 344.02 nm. These dominant emission bands indicate that the poly(3-octyl thiophene) was decomposed by plasma interaction. Nevertheless, the reaction between the polymer and nitrogen, hydrogen and air plasmas is more intense than that in the helium plasma. The possible reaction channels and formation mechanisms of some species produced are discussed. © 2007 Wiley Periodicals, Inc. J Appl Polym Sci 105: 2947–2954, 2007

Key words: optical emission spectroscopy; pulsed plasmas; poly(3-octyl thiophene)

INTRODUCTION

In situ optical emission spectroscopy provides information of decomposition processes with time exposure to gas plasma. Kumagai et al.[1] and Kobayashi et al.[2] have reported the decomposition of poly(ethylene terephthalate) and polyacrylonitrile polymers by plasma using emission spectroscopy analysis. The emission peaks obtained in pyrrole films indicate that the excited species do take part in the fragmentation mechanisms in plasma polymerization processes.[3]

Plasma is commonly employed as a deposition method of polymers (polymerization by plasma), as well as in surface treatments. Optical and electrical properties of plasma-polymerized pyrrole films have been previously studied.[3] Effects of such studies as a function of the temperature and the radio frequency (RF) had been done in plasma enhanced chemical vapor deposition (PECVD) of thiophene.[4] In addition, oxygen plasma treatment introduced oxygen-containing polar functional groups into the surface of the polystyrene and polydimethylsiloxane.[5] High intensity oxygen RF plasma treatment of polystyrene and polycarbonate was shown to result in surfaces highly stable toward washing, dry storage and heat treatment.[6] In these days, environmental pollution has become a global problem and plasma technology applied to toxic remainders treatment has attracted the attention of researchers. For this reason, degradation of many compounds has been investigated by plasma discharge.[7–9]

Polymer–plasma interaction generates chemical reactive species. This interaction can break the polymer bonds generating different fragments. Agostino et al.[10] observed, by emission spectroscopy, the production of chemical reaction because of the plasma-polymer interaction.

In spite of many researches that have been made to study polymer-surface modification and polymerization by plasma very little is known about plasma reaction processes. Additionally, gaseous pollution control, and solid and liquid waste treatments based on plasma have become significant, recently.[11,12] To improve this technology it is necessary the knowledge of the mechanisms involved in the degradation processes.

Up to we know, no emission spectroscopy analysis of poly(3-octyl thiophene) (P3OT)-plasmas interactions has been studied. The importance of the P3OT lie in the fact that it is applied as active layer in light-emitting diodes (LED)[13] and a *p*-type layer in photovoltaic heterojunctions.[14] Recently, TiO_2 : P3OT photovoltaic structure was obtained with a conversion efficiency of 0.17%.[15] Therefore, decomposition of P3OT and the formation of other species in environmental conditions (air atmosphere) attracted our

Correspondence to: Y. Rodríguez-Lazcano (yrl@fis.unam.mx).
Contract grant sponsor: DGAPA; contract grant numbers: IN-105707-3 and CONACyT 41,072-F.

Journal of Applied Polymer Science, Vol. 105, 2947–2954 (2007)

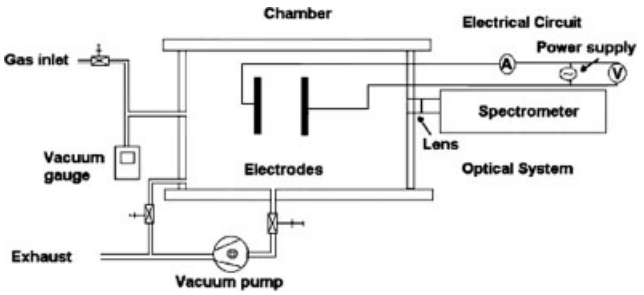

Figure 1 Schematic diagram of the experimental apparatus.

attention. In addition, these two processes are very important because as they are steps before polymerization and surface modifications, its knowledge can be useful to make them more efficient.

The aim of this work is to study the polymer-plasma reactions taking place in the decomposition process of poly(3-octyl thiophene) exposed to air. To compare nitrogen, hydrogen, and helium plasmas, we also used. Emission spectroscopy analysis is a common technique for the detection of chemical species in plasma. Possible mechanisms to obtain some of the species observed by emission spectroscopy are discussed.

EXPERIMENTAL

The experimental equipment to generate the pulse plasma was described in detail elsewere[16] and is shown in Figure 1. The system consists of two stainless steel circular plane electrodes, 3 mm thick and 30 cm in diameter. One of them has a 2.27 cm^3 receiver where the polymer of about 34 mg is put. The electrodes are positioned at the center of the reaction chamber. They have a gap spacing of 1 and 18 mm in the closer and wider distance, respectively. The gas was injected into the reaction chamber through the upper flange. The same gas connection was used for the pressure sensor MKS, Type 270 (USA). The pulsed plasma was produced in environments of helium, nitrogen, air, and hydrogen gas, respectively, all of them in ultra pure gas (Praxair 99.99%), at a pressure of 4.0×10^2 Pa during 90 min. The discharge power supply was maintained at an output of 220 V and a current of 0.2 A, which was measured using a digital Tektronic multimeter model DM2510 (USA). The base pressure of the plasma chamber (volume of 6.3×10^3 cm^3) was maintained at 0.5 Pa using a mechanical pump (Trivac D10, Leybold Pump (Germany) with nominal pumping speed of 3.3×10^{-3} m^3 s^{-1}) and purged with the working gas at a pressure of 1.3×10^2 Pa for several times to remove the background gas. The chamber was filled with the gas at the required working pressure. Under these conditions the background pressure was 0.12% of the working pressure.

A quartz window was installed on the right lateral flange to monitor the active species generated in the glow discharge by plasma emission spectroscopy. The glow discharge was focused at a right angle with respect to the center of the electrodes plane on the fiber optic entrance with 20 cm focal distance quartz lens; the exit of the optic fiber was connected to a high-resolution Ocean Optics Spectrometer Model HR2000CG-UV-NIR (USA) equipped with a 300 lines-mm^{-1} composite blaze grating giving a reciprocal linear dispersion of 0.45 nm mm^{-1}. The spectrum (200–600 nm) of the emission cell was recorded with an optic fiber connected to a UV2/OFLV-5 detector (2048-element linear silicon CCD array). The detector has a spectral response in the range of 300–600 nm with an efficiency >30%; the scan interval was 0.47 nm. The inlet and outlet slits were 5×10^3 nm wide. The data were obtained in a single accumulation of 10 s integration time, which corresponds to 600 times that of the period of pulse voltage. The lens and optic fiber assembly was movable to focus different points of the plasma discharge between the electrodes.

3-Octylthiophene (3OT) was synthesized through a Grignard reactive by coupling of octyl magnesium bromide (Aldrich, USA) with 3-bromothiophene (Aldrich, USA) in the presence of [1,3-bis(diphenylphospino)propane] nikel (II) chloride (Aldrich, USA). The final product, octylthiophene, was distilled under a reduced pressure of 467 Pa at 120°C. The poly(3-octyl thiophene)[17,18] ($C_{12}H_{21}S$, Fig. 2 shows the chemical structure) was obtained by direct oxidation of 3OT using $FeCl_3$ (Aldrich, USA) as oxidant/catalyst. Anhydrous $FeCl_3$ (0.0243 mol) dissolved in dried $CHCl_3$ (J. T. Baker, USA) was slowly added to 6.62×10^{-3} mol of distilled 3OT dissolved in dried $CHCl_3$. The reaction mixture was stirred at room temperature for 24 h. The product was precipitated in methanol (J. T. Baker, USA), filtered with a Buchner funnel and carefully washed with methanol, hydrochloric acid (10 vol %) (J. T. Baker, USA) and acetone (J. T. Baker, USA). The final black P3OT product was then dried. ATR absorption spectrum for the polymer was obtained in a Nicolet FTIR Spectrometer, model 680 (USA) and is shown in Figure 3. The IR stronger absorptions were identified. The peaks at 2929 and 2851 cm^{-1} correspond to the C—H stretching modes. The stronger bands at 1293, 1146, and 1075 cm^{-1} can be assigned to various stretching modes of the thiophene ring; symmetric,

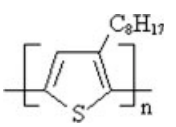

Figure 2 Chemical structure of poly(3-octyl thiophene).

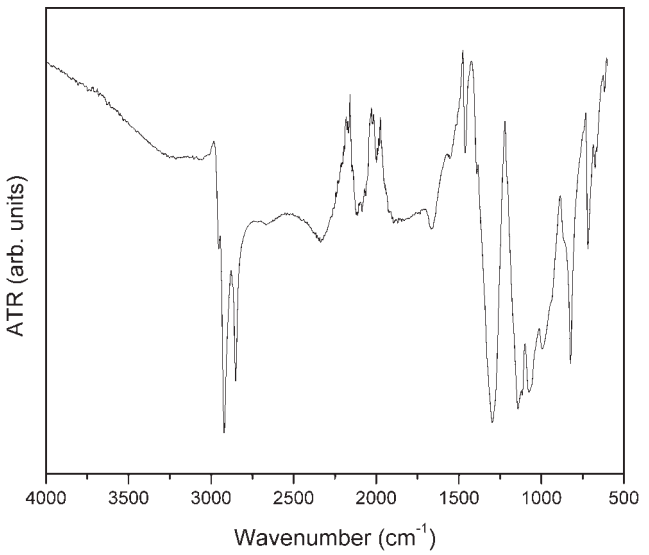

Figure 3 ATR spectrum of poly(3-octyl thiophene).

intraring and interring, respectively. The peak at 828 cm^{-1} is assigned to the C—S stretching vibration. Absorption at 723 cm^{-1} is produced because of C—H deformation of the methylene group of the octyl chain.

RESULTS AND DISCUSSION

In situ emission spectroscopy analysis for poly(3-octyl thiophene)-plasmas decomposition processes

The poly(3-octyl thiophene) (P3OT) was exposed in helium, nitrogen, air and hydrogen plasmas, respectively, during 90 min. The optical emission was measured at 1, 5, 10, 15, 20, 25, 30, 45, 60, 75, and 90 min. The evolution of the emission lines of the P3OT-plasma systems as a function of the gas plasmas used is shown in Figure 4 at a discharge time of 30 min. In the 200–600 nm wavelengths region, several emission peaks were observed and assigned.[19,20]

The stronger lines and bands identified for polymer-plasmas interaction are summarized in Table I. For nitrogen, air and hydrogen plasmas, all lines and bands showed in Table I are presented, except He I. In the case of poly(3-octyl thiophene) with nitrogen and air interaction, additional emissions corresponding to CN^+, CN, and C_2N were observed because of the reaction of nitrogen with the species formed by the decomposition of the polymer. N_2 (second positive system) and N_2^+ (first negative system) are also present in the spectra. These emission bands are shown in Table II. Some of the bands corresponding to the second positive and the first negative systems are more intense in air plasma. The result come from the match of nitrogen emission with some emissions corresponding with oxygen or oxygen compounds, suggesting the reaction of this gas with the species formed from the polymer decomposition. We observed that some second positive system bands match with O_2 (314.5 and 406.4 nm), CO_2^+, CHO, and NCO and the first negative line at 354.31 nm matches with O_2. The match causes the superposition of the intensities. Table III shows the additional bands. An increase in the peak centered at ~427.96 nm is observed in air and nitrogen plasmas due the match of C_2 (426.62 nm) with N_2.

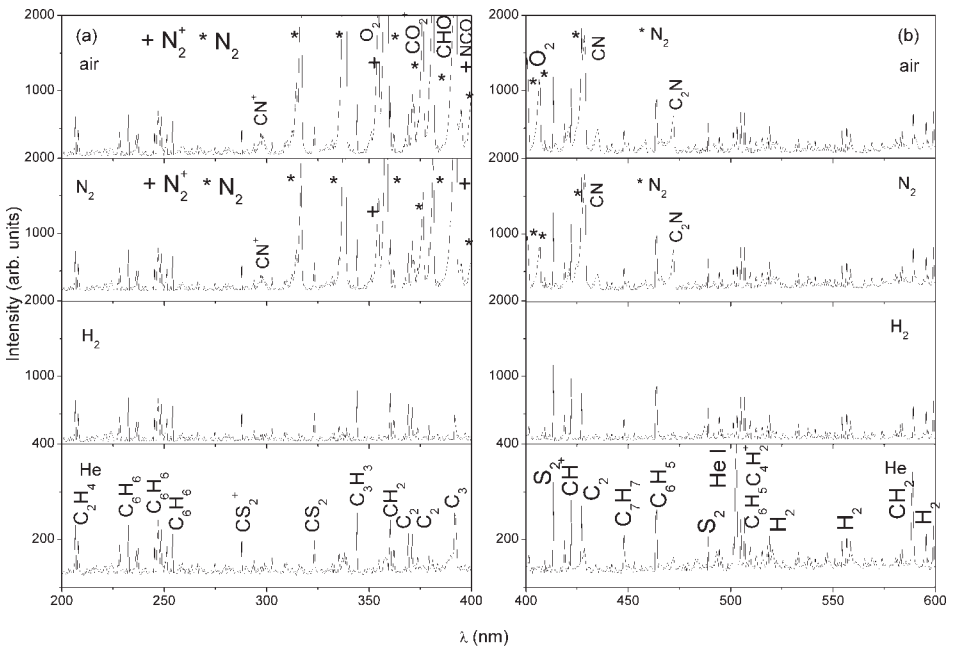

Figure 4 Emission spectra in different plasmas at 30 min from (a) 200–400 nm and (b) 400–600 nm.

TABLE I
Assignments of Emission Spectra Lines and Bands Observed in Helium, Air, Nitrogen, and Hydrogen Plasma [19,20]

Species	Transitions	Wave length (nm)
C_2H_4 (ethylene)		206.65
C_6H_6 (benzene)		231.94
		246.55
CS_2^+		288.10
CS_2		322.65
C_3H_3 (propargyl radical)		344.02
CH_2 (methylene radical)		360.04
		589.32
C_2	$(c^1\Pi_g - b^1\Pi_u)$	368.42
	$(c'^1\Pi_g - b^1\Pi_u)$	370.84
	$(A^3\Pi_g - X'^3\Pi_u)$	426.62
C_3		391.99
S_2	$(B^3\Sigma_u^- - X^3\Sigma_g^-)$	413.35
	$(B^3\Sigma_u^- - X^3\Sigma_g^-)$	489.34
CH^+	$(A^1\Pi - X^1\Sigma)$	422.51
C_7H_7 (benzyl radical)		447.91
C_6H_5 (phenyl radical)		464.05
		505.26
He[a]		502.64
$C_4H_2^+$		506.68
H_2		518.67
		557.26
		595.97

[a] It was not present in nitrogen, air, and hydrogen plasmas.

Figure 5 shows the time profile of emission intensity of S_2 band at 413.35 nm produced in different plasma gases. The values of the intensity are very close in nitrogen, hydrogen and air plasmas, but for helium plasma the intensity is less. The same behavior is observed for all the lines analyzed. A loss of ~15% of the weight in nitrogen, hydrogen and air plasmas was found. On the other hand, no loss of weight was observed in the helium atmosphere.

TABLE II
Additional Emission Spectra Bands Observed in Air and Nitrogen Plasmas [19,20]

Species	Transitions	Wave lengh (nm)
CN^+	$(c^1\Sigma - a^1\Sigma)$	295.94
CN	$(B^2\Sigma - A^2\Pi)$	426.60
C_2N	$(A^2\Delta - X^2\Pi)$	472.01
N_2[a]	$(C^3\Pi_u - B^3\Pi_g)$	315.67
		337.56
		357.97
		376.01
		381.30
		399.50
		406.59
		426.66
N_2^+[b]	$(B^2\Sigma_u^+ - X^2\ \Sigma_g^+)$	354.31
	$(B^2\Sigma_u^+ - X^2\ \Sigma_g^+)$	392.42

[a] Second positive system.
[b] First negative system.

TABLE III
Additional Emission Spectra Bands Observed in Oxygen Plasma [19,20]

Species	Transitions	Wave lengh (nm)
O_2	$(B^3\Sigma_u^- - X^3\Sigma_g^-)$	314.50
	$(A^3\Sigma_u^+ - X^3\Sigma_g^-)$	354.20
	$(A^3\Sigma_u^+ - X^3\Sigma_g^-)$	406.40
CO_2^+	$(A^2\Pi - X^2\Pi)$	376.10
CHO		382.00
NCO		399.20

These results suggest that in air, nitrogen and hydrogen atmospheres the poly(3-octyl thiophene) is etched. In addition, these gasses react with the polymer and favor the reaction processes. The time profile of the lines and bands was constant as a function of the time discharge. This is probably due to a geometrical effect of the gas interacting with the polymer surface.

Proposed mechanisms for poly(3-octyl thiophene)-plasmas decomposition processes

To present an analysis of kinetic processes in the polymer-glow discharge interaction, the influence of electron impacts, the vibrational kinetic and physical–chemical reaction have to be taken into account. The reactions include electron-neutral, ion-neutral and neutral-neutral interactions. Possible mechanisms to obtain some of the species observed by emission spectroscopy are discussed below and summarized in Table IV.

The interaction plasma - polymer produces the decomposition of the poly(3-octyl thiophene). Several species can be produced directly by the interaction between the electrons and the polymer. For example,

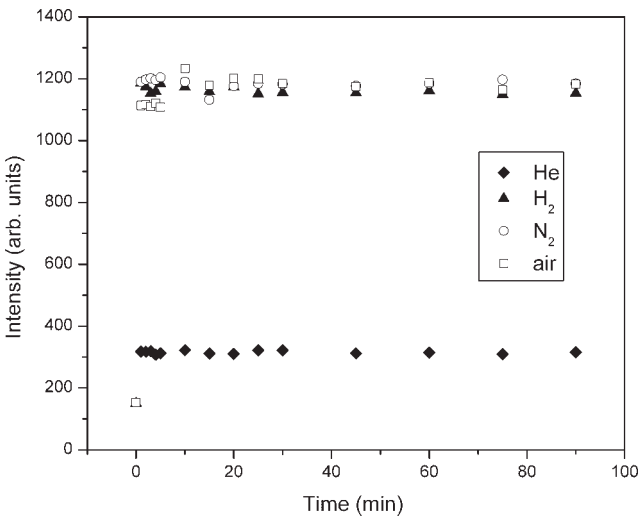

Figure 5 Time profile of emission intensities of S_2 line (413.35 nm) at the different plasma gases.

TABLE IV
Possible Mechanisms for the Formation of the Species Observed by Emission Spectroscopy

R.	Species	Process	Ref.
R1	$C_4H_2^+$	$C_2H_2 + C_2H_2^+ \rightarrow H_2 + C_4H_2^+$	[21]
R2	CH_2	$CH + H_2 \rightarrow CH_2 + H$	[21]
R3		$O(^3P) + C_2H_4 (X^1A_g) \rightarrow H_2CO (X^1A_1) + CH_2 (X^3B_1)$	[22]
R4		$O(^3P) + C_2H_4 (X^1A_g) \rightarrow CH_2 (^1A_1) + H_2CO$	[22]
R5	HCO	$O(^3P) + C_2H_4 (X^1A_g) \rightarrow CH_3 (X^2A_2'') + HCO (X^2A')$	[23]
R6		$CH_3 + O \rightarrow H_2 + HCO$	[24]
R7		$CH_3 + O_2 \rightarrow CH_3O_2 \rightarrow H_2O + HCO$	[25]
R8	C_2H_4	$C_2H_3 + CH_3 \rightarrow C_2H_4 + {}^3CH_2$	[26]
R9	CN	$C_2 (a^3\Pi) + NO (X^2\Pi) \rightarrow CN (A^2\Pi, B^2\Sigma) + CO (X^1\Sigma)$	[27]
R10	C_2N	$C_2 (a^3\ \Pi_u) + NO \rightarrow C_2N + O$	[28]
R11	NCO	$CH (X^2\Pi) + NO (X^2\Pi) \rightarrow H (^2S) + NCO (X^2\ \Pi, A^2\ \Sigma^+)$	[29]
R12		$CO^+ + N_2 \rightarrow N^+ + NCO$	[30]
R13		$N_2{}^+ + CO \rightarrow N^+ + NCO$	[30]
R14		$CN + O_2 \rightarrow NCO + O$	[31]
R15	C_6H_6	$C_3H_3 + C_3H_3 \rightarrow C_6H_6$	[32]
R16		$C_6H_5 + H \rightarrow C_6H_6$	[32]

CH^+, CH_3, C_2H_3 are easy to obtain because of the decomposition of the poly(3-octyl thiophene) because of its chemical structure. Nevertheless, species like CH_3 and C_2H_3 were not observed in the emission spectroscopy because they react to form other species (R8). Many different species are produced by collisions between free electrons generated, by the ionization of the gas, and the polymer. Electrons in a nonthermal plasma, like a glow discharge, have an energy of up to 3.2×10^{-18} J,[33] enough to brake the chemical bonds and release the species in the gas phase. These chemical species are ions, radicals; and atoms and molecules in the ground state and in excited levels. These active species can react among them producing other species or intermediate complexes, like in reactions R3–R5 and R15.

Some of the species observed by emission spectroscopy have been detected by mass spectroscopy.[34] Decomposition of the thiophene produces directly the propargyl radical with the 19.7% of the total intensity. Nevertheless, other species obtained by mass spectroscopy like HCS (34.9%) or C_2SH_2 (54.1%) are no observed by optical emission probably because their decomposition because of poly(3-octyl thiophene)-plasma interaction. In addition, species like $C_4H_2^+$, C_2, and CH^+ are presented by mass spectroscopy with very little intensity, but their interaction with the plasma increases their intensity by optical spectroscopy.

The species in which the gases are decomposed by the ionization process, for example N_2 and N_2^+ in a nitrogen plasma, and O_2 and O_2^+ in an oxygen plasma, can react with the polymer generating other species. The presence of nitrogen and air in the chamber produce the reaction between the originating species of the gas and the poly(3-octyl thiophene), and the formation of CN, CN^+, and C_2N, and CO_2^+, NCO, HCO, respectively. Since helium is an inert gas it does not react with the poly(3-octyl thiophene) and only decomposition by electrons-polymer interactions are presented (Fig. 4). The species observed in helium are presented in hydrogen plasma with high intensity, but no other species were form.

The production of some species can be explained as follow:

- Population of $C_4H_2^+$

  One of the most important ionic species in acetylene plasma is $C_4H_2^+$. Herrebout et al.[21] developed one-dimensional fluid model for an RF acetylene discharge. The $C_4H_2^+$ specie can be obtained through the reaction channel R1. This ion-neutral reaction has a reaction rate coefficient of 1.0×10^{-15} m^3 s^{-1}.[21]
- Population of CH_2

  In acetylene plasma the CH_2 radical specie presents high density. This specie can be formed through the neutral–neutral reaction R2 with a reaction rate coefficient of 6.8×10^{-19} m^3 s^{-1}.[21] The $O(^3P) + C_2H_4$ reaction (R3) plays an important role in C_2H_4/O_2 flames and in hydrocarbon combustion in general.

  Oxygen atoms in their triplet ground electronic state undergo an electrophilic addition onto the C=C bond, forming adducts that are vibrationally excited triplet biradicals corresponding to the spin-conservation rule ($O(^3P) + C_2H_4 (X^1A_g) \rightarrow CH_3CHO (X^1A')$). The triplet biradicals either decompose to products (by H- or CH_2-loss) or carry out intersystem crossing (ISC) to singlet biradicals. Finally, the singlet biradicals produced from the triplet adducts upon ISC may either convert to ''hot'' epoxides by ring

closure or rearrange by internal migration of H atoms or alkyl groups into ''hot'' carbonyl compounds. These ''hot'' compounds may undergo collisional stabilization under high-pressure reaction conditions. In this case $^{o}CH_2—CH_2—O^{o}$ (C_1, ^3A) can dissociate by breaking the C—C bond as shown in R3, facing a barrier of 92 kJ/mol[22] or into $CH_2(^1A_1)$ + H_2CO products (reaction R4) without exit barrier. This is one of the major possible primary product channels with experimental reaction enthalpy ($\Delta_r H(0K)$) of −23 and −29 kJ/mol obtained by quantum chemical calculations.[22]

- Population of HCO

  The HCO specie can be produced by different channels, such as R5. It has experimental $\Delta_r H$ of −117 kJ/mol, whereas by quantum chemical calculations the value is −121 kJ/mol.[22] Triplet $CH_3—^{o}CH—O^{o}$ (C_1, ^3A) can decompose via different channels, but the decomposition into CH_3 + CHO is predominant because of its lower barrier height of 54 kJ/mol. The CH_3 + CHO products were observed in molecular beam experiments under collision-free conditions.[23] The CH_3CHO can directly decompose into CH_3 + CHO, variational transition states without exit barriers.[22]

  Another possible channel for the HCO formation is through the exothermic reaction R6 with ΔH of −352 kJ/mol.[24] This theoretical result obtained by Marcy et al.[24] represent the possibility of CH_3O intermediate complex formation, as well as, the H + H_2CO intermediate step.

  The oxidation of CH_3, the most stable alkyl radical, by molecular oxygen is one of the most important reactions in the combustion of hydrocarbons. This reaction has been investigated by *ab initio* molecular orbital theory and variational transition state theory calculations.[25] The most exothermic products, CHO + H_2O (reaction R7) were found to be kinetically inaccessible because of the larger barrier, 198 kJ/mol above the reactants.[25]
- Population of C_2H_4

  Radical-radical cross-combination reactions constitutes an integral part of the overall mechanisms of oxidation and pyrolysis of hydrocarbons. The C_2H_4 specie can be obtained through reaction R8 with ΔH^{o}_{298} = −5 kJ/mol.[26] Sotoliarov et al.[26] studied this system by quantum chemical methods. The estimate of the barrier for the direct reaction is very high, ~45 kJ/mol.
- Population of CN

  The population of CN can be explained through reaction R9. The reaction between C_2 and NO is of interest to NO reburning for the reduction of NO_x emissions from combustion. This reaction was studied in a high-temperature photochemistry reactor.[35] This reaction has been observed to produce CN(B-X) Violet System and CN(A-X) Red System chemiluminescence, with ΔH^{o}_{298} of −501 and −303 kJ/mol, respectively, for A and B states formation.[27] This is a direct reaction, in the sense that the CN is not produced from the possible intermediates C_2O or C_2N.[28]
- Population of C_2N

  C_2N can be produced by reaction R10. Kruse and Roth[36] studied the C_2 + NO system in a shock tube from 3150 to 3950 K at pressures from 1.6 to 2.2 × 10^8 Pa. The most likely C_2N product of C_2 collisions with NO is CCN.[35] Reisler et al.[28] suggested that initially only one bond is formed and subsequently the C_2NO (or presumably also C_2ON) complex rotates and rearranges itself so that a second bond is formed and the products separate.
- Population of NCO

  The cyanato radical NCO is a very important intermediate in the combustion chemistry of nitrogenous fuels, and the knowledge of its heat of formation is important for kinetic modeling of the processes for reduction of NO_x from combustion exhausts. NCO was obtained from a pure and highly intense CH beam source by use of the $C(^1D)$ + H_2 reaction with the combination of the state selection and purification by an electrostatic hexapole field, through R11 with ΔH_{298} = −333 kJ/mol.[29] Nagamachi et al.[29] obtained a dependence of the state-resolved reaction cross section with the CH rotational state.

  The chemistry of CO, N_2 and their ions is important in combustion systems, planetary atmospheres, and interstellar clouds. Reactions R12 and R13 were performed in an ion-molecule reaction mass spectrometer with heats of formation ($\Delta_f H^{o}(NCO)$) of 126 and 132 kJ/mol, respectively.[30] The experimental dissociation energy for $(N_2\text{-}CO)^+$ is (66 ± 18) kJ/mol,[30] while theoretical calculation give values of 59 and 54 kJ/mol. The large binding energy is explained by the resonance interaction between the two charge transfer states CO^+-N_2^+. This suggests that the initial collision leads to the same intermediate complex $(N_2—CO)^+$, if one starts from CO^+ + N_2 or N_2^+-CO.

  The NCO radical can be synthesized by reaction R14 in interstellar clouds. Prasad[31] reported a theoretical study of the electric and magnetic hyperfine coupling constants of ^{14}N in NCO and CNO radicals in $X^2\Pi$, $A^2\Sigma^+$, $B^2\Pi$, and $2^2\ \Sigma^+$ states.
- Population of C_6H_6

  Miller et al.[32] proposed a model for describing the rate coefficient and product distribution of

the reaction between two propargyl radicals (reaction R15) for use in flame modeling, were one of the most stable products is benzene. Another way for the formation of benzene, proposed by the same authors, is the reaction between C_6H_5 and H (R16), with enthalpy of 574 kJ/mol.

The vibrational excitation of H_2 molecules enhances the reaction probability in the $H_2 + C_2H$ system.[37] The calculations were done for the first four vibrational excitations of H_2 (υ_1, $j_1 = 0$). In general, the vibrational excitation of υ_1 enhances the reactivity of this reaction. First, the vibrational excitation of υ_1 enhances the reactivity by lowering the reaction threshold as υ_1 increases. Second, the vibrational excitation reaction of υ_1 enhances the reactivity by increasing the probability amplitude dramatically as υ_1 increases. In addition, resonance structures are found in these reactions probably at relatively low kinetic energies. These results indicate that dynamical resonances can be produced in systems involving hydrogen. At higher kinetic energies, the collision time is much shorter than that at lower kinetic energies, the H_2 molecule must rotate itself fast enough to find the right position to combine with the C atom in C—CH so the reaction occurs. The fast rotation allows it to have more chances, during the shorter collision time, to reorientate itself to the suitable position to attach with the C atom in C—CH. On the other hand, the product channels in the reaction of H_2CO^+ with C_2H_2 depend on the collision energy and H_2CO^+ vibrational excitation.[38] The electron impact dissociation of N_2O into N_2 and $O(^3P)$ is much more significant than the other channels because the N_2O dissociation cross section is higher than the other ones.[39]

CONCLUSIONS

The emission lines and bands observed due to the interaction of poly(3-octyl thiophene) with nitrogen, helium, hydrogen and air plasmas were identified. The stronger emission bands were assigned to C_3H_3 at 344.02 nm, S_2 ($B^3\Sigma_u^- - X^3\Sigma_g^-$) at 413.35 nm, CH^+ ($A^1\Pi - X^1\Sigma$) at 422.51 nm and CH_2 at 589.32 nm. Bands corresponding to CN^+ ($c^1\Sigma - a^1\Sigma$) at 295.94 nm, CN ($B^2\Sigma - A^2\Pi$) at 426.6 nm and C_2N ($A^2\Delta - X^2\Pi$) at 472.01 nm were obtained due to the interaction of poly(3-octyl thiophene) with nitrogen and air plasmas. On the other hand, the interaction with the oxygen in the air plasma produces the increase in the intensity of some bands because it matches with some compounds of oxygen, like CO_2^+ ($A^2\Pi - X^2\Pi$) at 376.1 nm, CHO at 382.0 nm, and NCO at 399.2 nm. A loss in the polymer weight of approximately 15% was obtained in nitrogen, hydrogen and air plasmas because of the reaction of these gases with the polymer. In addition, the intensity of the stronger lines in these plasmas is four times larger than in helium. These results suggest that nitrogen, helium, hydrogen and air plasmas attacked the polymer, decomposing it. Whereas, in nitrogen, hydrogen and air plasmas different reactions between the polymer and the plasmas produce several species. Time profiles of those emission transitions suggest no changes in the intensity probably because a geometrical effect of the gas interacting with the polymer surface.

Some mechanisms are proposed for the species formation. Species like CH^+, CH_3, C_2H_3 can be formed directly because of the interaction of the electrons with the polymer. Others can be formed trough the reactions of ions and radicals coming from the polymer. In addition, the interaction with the nitrogen and air plasmas can produce other species like CN and HCO, because of the reaction processes that take place in the polymer-plasma surface.

The authors are grateful to Armando Bustos, Anselmo González, and José Rangel for technical assistance; also we are grateful to B. E. Fuentes and F. Castillo for helpful suggestions and comments. We want to thank to C. López-Mata for the polymer preparation.

References

1. Kobayashi, T.; Sasama, T.; Wada, H.; Fujii, N. J Vac Sci Technol A 2001, 19, 2155.
2. Kumagai, H.; Hiroki, D.; Fujii, N.; Kobayashi, T. J Vac Sci Technol A 2003, 22, 1.
3. Kumar, D. S.; Nakamura, K.; Nishiyama, S.; Ishii, S.; Noguchi, H. J Appl Phys 2003, 93, 2705.
4. Kim, M. C.; Cho, S. H.; Han, J. G.; Hong, B. Y.; Kim, Y. J.; Yang, S. H.; Boo, J. H. Surf Coat Technol 2003, 169, 595.
5. Marukami, T.; Kuroda, S.; Osawa, Z. J Colloid Interface Sci 1998, 202, 37.
6. Larsson, A.; Derand, H. J Colloid Interface Sci 2002, 246, 214.
7. Gai, K. J Chin Chem Soc 2006, 53, 627.
8. Lukes, P.; Clupek, M.; Sunka, P.; Peterka, F.; Sano, T.; Negishi, N.; Matsuzawa, S.; Takeuchi, K. Res Chem Int 2005, 31, 285.
9. Amano, R.; Tezuka, M. Water Res 2006, 40, 1857.
10. d'Agostino, R. Plasma Deposition, Treatment and Etching of Polymers; Academic Press: New York, 1990.
11. Chang, J. Sci Technol Adv Mater 2001, 2, 571.
12. Abdelmalek, F.; Gharbi, S.; Benstaali, B.; Addou, A.; Brisset, J. L. Water Res 2004, 38, 2339.
13. Singh, T. B.; Waghmare, U. V.; Narayan, K. S. Phys Lett 2002, 80, 1213.
14. Manoj, A. G.; Narayan, K. S. Opt Mater 2002, 21, 417.
15. Slooff, L. H.; Wienk, M. M.; Kroon, J. M. Thin Sold Films 2004, 451, 634.
16. Martínez, H.; Rosales, I. Surf Eng 2005, 21, 139.
17. Nicho, M. E.; Hu, H.; López-Mata, C.; Escalante, J. Sol Energy Mater Sol Cells 2004, 82, 105.
18. López-Mata, C.; Nicho, M. E.; Hu, H.; Cadenas-Pliego, G.; García-Hernández, E. Thin Solid Films 2005, 490, 189.
19. Pearse, R. W. B.; Gaydon, A. G. The Identification of Molecular Spectra; Chapman and Hall: London, 1963.

20. Striganov, A. R.; Odintsova, G. A. Tables of atomic and Ionic Spectral Lines; Energoatomizdat: Moscow, 1982.
21. Herrebout, D.; Bogaets, A.; Gijbels, R.; Goedheer, W. J.; Vanhulsel, A. IEEE Trans Plasma Sci 2003, 31, 659.
22. Nguyen, T. L.; Vereecken, L.; Hou, X. J.; Nguyen, M. T.; Peeters, J. J Phys Chem A 2005, 109, 7489.
23. Schmoltner, A. M.; Chu, P. M.; Brudzynski, R. J.; Lee, Y. T. J Phys Chem 1989, 91, 6926.
24. Marcy, T. P.; Diaz, R. R.; Heard, D.; Leone, S. R. J Phys Chem A 2001, 105, 8361.
25. Zhu, R.; Hsu, C. C.; Lin, M. C. J Chem Phys 2001, 115, 195.
26. Stoliarov, S. I.; Knyazev, V. D.; Slagle, I. R. J Phys Chem A 2002, 106, 6952.
27. Reisler, H.; Mangir, M.; Witting, C. J Phys Chem 1980, 73, 2280.
28. Reisler, H.; Mangir, M.; Witting, C. J Phys Chem 1979, 71, 2109.
29. Nagamachi, Y.; Ohoyama, H.; Ikejiri, K.; Kasai, T. J Chem Phys 2005, 122, 064307–1.
30. Lu, W.; Tosi, P.; Bassi, D. J Chem Phys 2000, 113, 4132.
31. Prasad, R. J Chem Phys 2004, 122, 10089.
32. Miller, J. A.; Klippenstein, S. J. J Chem Phys A 2003, 107, 7783.
33. Boening, H. V. Plasma Science and Techonology; Cornell University Press: New York, 1982.
34. Wasada, N. Available from the National Institute of Advanced Industrial Science and Technology (AIST), Spectral Database for Organic Compounds SDBS. http://www.aist.go.jp/RIODB/SDBS/cgi-bin/cre_index.cgi.
35. Ristanovic, A.; Fernandez, A.; Fontijn, A. J Phys Chem A 2002, 106, 8291.
36. Kruse, T.; Roth, P. Int J Chem Kinet 1999, 31, 11.
37. Wang, D. J Chem Phys 2005, 123, 194302–1.
38. Liu, J.; Devender, B.; Anderson, S. C. J Chem Phys 2005, 123, 204313–1.
39. Date, L.; Radouane, K.; Despax, B.; Yousif, M.; Caquineau, H.; ad Hennand, A. J Phys Part D: Appl Phys 1999, 32, 1478.